

## EUROfusion / Work Programme 2015 Enabling Research

Project: **Fast Model Predictive Control for Magnetic Plasma Control**



Deliverable D1:

### **A set of reduced-order models and a state-estimation scheme for ITER plasma shape and current control**

Date due: 30.6.2015

Samo Gerškšič, Boštjan Pregelj, Andrej Debenjak <sup>a</sup>

Gianmaria De Tommasi, Marco Ariola, Alfredo Pironti, Massimiliano Mattei <sup>b</sup>

<sup>a</sup>Jožef Stefan Institute, Jamova 39, Ljubljana, Slovenia

<sup>b</sup>Associazione EURATOM-ENEA-CREATE, Univ. di Napoli Federico II, Via Claudio 21, 80125, Napoli, Italy



This work has been carried out within the framework of the EUROfusion Consortium and has received funding from the European Union's Horizon 2020 research and innovation programme under grant agreement number 633053. The views and opinions expressed herein do not necessarily reflect those of the European Commission.

# Contents

1	Introduction.....	4
2	Magnetic plasma control simulation setup.....	5
2.1	Simulation models.....	5
2.2	Reference control scheme .....	6
3	Vertical stabilisation .....	8
4	MPC Plasma current and shape (CSC) controller .....	8
5	Model preparation for KF and MPC .....	10
6	KF tuning .....	13
7	Conclusions.....	18

# Summary

Plasma magnetic control schemes typically consist of a cascade control scheme with a plasma current and shape controller (CSC) in the outer loop and a vertical stabilisation (VS) controller in the inner loop. The main challenges to tackle are: suppression of plasma shape transients after disturbances specific to tokamak reactors; robustness to changes in the plant dynamics; best possible use of the available chamber volume, so that the plasma is placed as close as possible to the plasma facing components; and tight control complying with the power supply and gap constraints. Model predictive control (MPC) is an advanced process control approach for dealing with constraints, already established in a range of industries involving multivariable processes with slower dynamics.

The aim of the MFPCFMPC project is to design a practically feasible MPC controller for the ITER CSC, which will be able to improve control in the presence of constraints on process signals.

This report covers the introductory part of the project, where the simulation setup is defined, a set of models for control design and analysis is prepared, and a state-estimation scheme for the MPC CSC control is prepared.

# 1 Introduction

In a magnetically confined fusion reactor, the plasma current and shape controller (CSC) is the component of plasma magnetic control (PMC) that determines the voltages applied to the poloidal field coils, to control the coil currents and the plasma parameters, such as the plasma shape, current, and position. In case of elongated, and hence vertically unstable plasmas, the CSC acts on the system already stabilised by the inner vertical stabilisation (VS) controller. The task of PMC is to maintain the prescribed plasma shape and plasma-wall distances (gaps), in presence of disturbances, such as vertical displacement events (VDE), H-L transitions or edge-localised modes (ELM), and to changes of local dynamics in different operating points [1, 2]. In order to achieve high performance, control methods that would improve the performance near the vessel boundaries and the actuator constraints are desired.

Model Predictive Control (MPC) is an established advanced process control approach in the process industry. It has gained wide industrial acceptance by facilitating a systematic approach to control of large-scale multivariable systems, with efficient handling of constraints on process variables and enabling plant optimisation [3]. These advantages are considered beneficial for CSC, and potentially also for other control systems of a tokamak. The main obstacle to using MPC for control of such processes is the restriction of the most relevant MPC methods to processes with relatively slow dynamics due to the long achievable sampling rates, typically needed for the on-line optimisation. However, speeding up MPC has been a topic of intensive research recently [4, 5, 6].

Modern MPC methods are based on state-space models, where model order is an important consideration. Plasma modelling procedures based on first principles result in models of very high orders [9], which are not convenient for control, and model reduction techniques are required to obtain models used for MPC design, in order to reach a manageable computational demand and numerical conditioning. The model order cannot be reduced arbitrarily, because it is important that the models retain a sufficiently accurate description of model dynamics; on the other hand, a high model order may also result in over-fitting to specific local dynamics that may actually result in poor robustness to changes of operating conditions. A set of models for different operating points of the ITER scenario is required for assessment of robustness of the controller to model inaccuracy.

An MPC scheme involving a steady-state target calculator (TC) and a dynamic controller (DC) for transient dynamics is being considered for implementation. For such MPC schemes it is particularly important that the model is also accurate in the low-frequency region.

Plasma models involve a large number of states that are not measurable. In state-space MPC approaches it is commonplace to use a linear observer or state estimator (Kalman filter) to estimate model states from the applied inputs and the measured outputs. Conceptually it would be appropriate to use a moving-horizon state estimator, which may also consider constraints just like the MPC controller, however the constrained state estimation task is computationally even more challenging than constrained control.

Due to the superconductive actuators, the plasma models for CSC control contain integrating dynamics (with poles at the origin), which requires special attention in the estimator implementation. Simple disturbance modelling using an open-loop observer with an output step disturbance model, which is frequently employed in simple industrial MPC methods, results in internal instability of the system, where internal signal values in the model may slowly diverge and eventually reach overflow. This problem is avoided by using a closed-loop estimator and by a proper choice of a disturbance model.

This report presents the concept of the plasma control simulation setup for the ITER CSC control problem, including a set of plasma models used for both plasma linear simulations and controller design, a set of disturbances expected to affect CSC control, a reference "conventional" control scheme including VS scheme based on [8], also intended to be used with MPC, and an alternative CSC based on singular perturbation decomposition (SPD) [7], and a state estimation scheme required for MPC CSC implementation.

## 2 Magnetic plasma control simulation setup

### 2.1 Simulation models

The simulations and controller design methods are based on high-order local linear dynamical models of the tokamak plasma from CREATE-L or CREATE-NL [9, 10] nonlinear equilibrium codes, at several different operating points for ITER plasma Scenario 1. The models are listed in Table 1. The model codes coincide with the time into the scenario. Initially, three different models were considered. Additional models were added in order to examine the effects of rapid changes of dynamics during L-H and H-L transitions, where closed-loop control with the reference control scheme is used. They may be used to assess the validity of simulation of such disturbances using a single linear model. The control design may be eventually validated with nonlinear simulations with the CREATE-NL model, but linear models are required for nominal control design and for fast performance assessment (nonlinear simulations are time consuming and may be affected by numerical issues).

Table 1. Local linear dynamic models.

Model code	Disturbance
t80	No disturbance
t90	No disturbance
t520	No disturbance
t079d50	L-H transition
t080d50	L-H transition
t081d50	L-H transition
t083d00	L-H transition
t085d00	L-H transition
t090d00	L-H transition
t529d50	H-L transition
t530d50	H-L transition
t531d00	H-L transition
t531d50	H-L transition
t532d00	H-L transition
t532d50	H-L transition

The models may be used to simulate disturbances specific to tokamak reactors. A Vertical displacement event (VDE) of a given amplitude may be simulated by initializing the simulation with an appropriate non-zero initial state of the plasma model. Several other types of disturbances may be simulated by injecting precomputed trajectories of  $\beta_p$  and  $I_i$

exogenous inputs to the plasma model: Minor disruption, Uncontrolled ELM, L-H transition, H-L transition. Some of these disturbances are relevant only at specific time into the pulse, therefore with specific local linear models.

## 2.2 Reference control scheme

As a reference control scheme, the Matlab/Simulink simulation scheme "v2d0" of CREATE is used. The scheme is displayed in Fig. 1, and the Plasma Model block is expanded in Fig. 2. The shown scheme is slightly modified to use the "absolute" values of the control signals rather than the "delta" differential values, relative to the operating point of the local linear model.

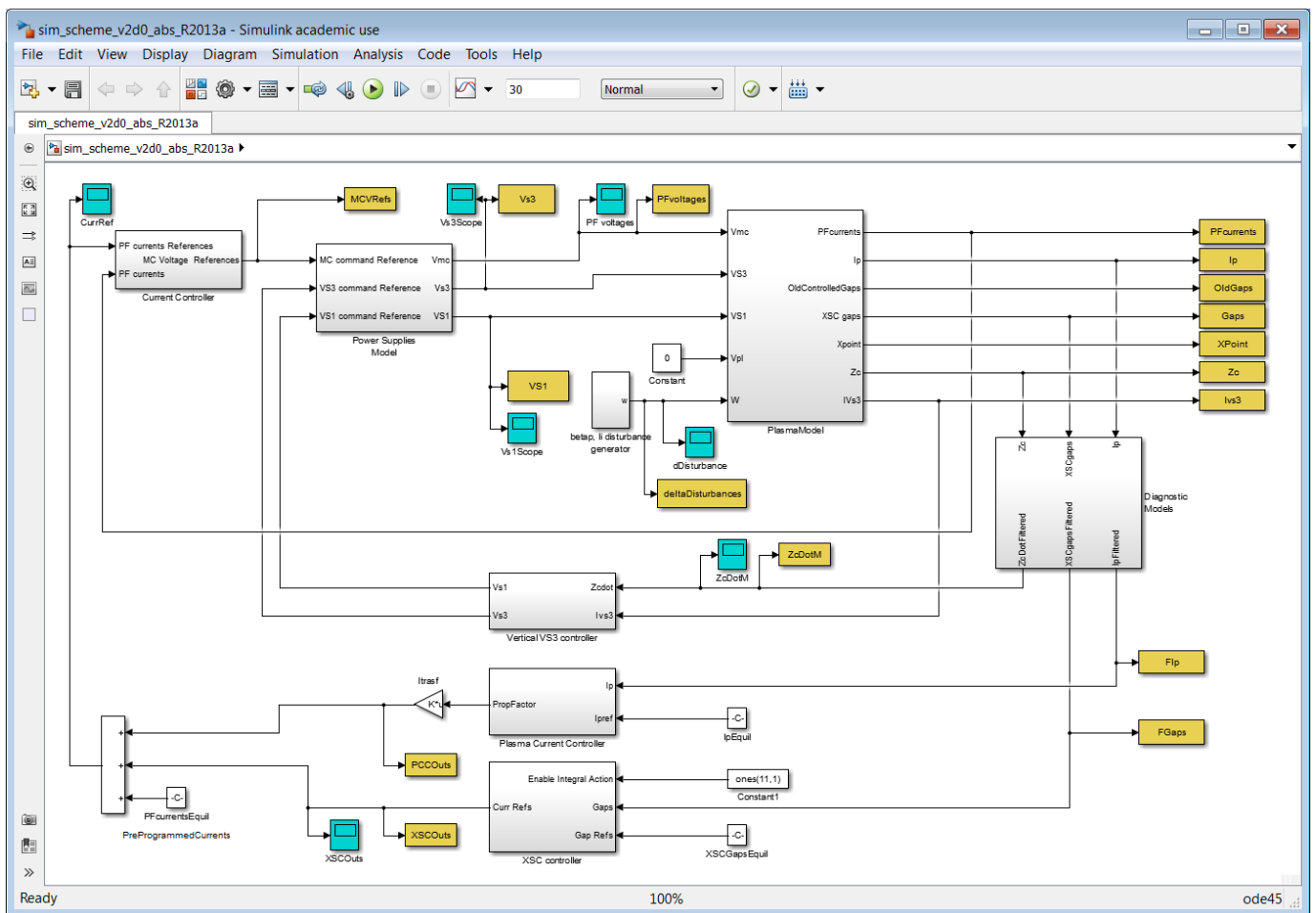


Fig. 1. Reference simulation control scheme "v2d0".

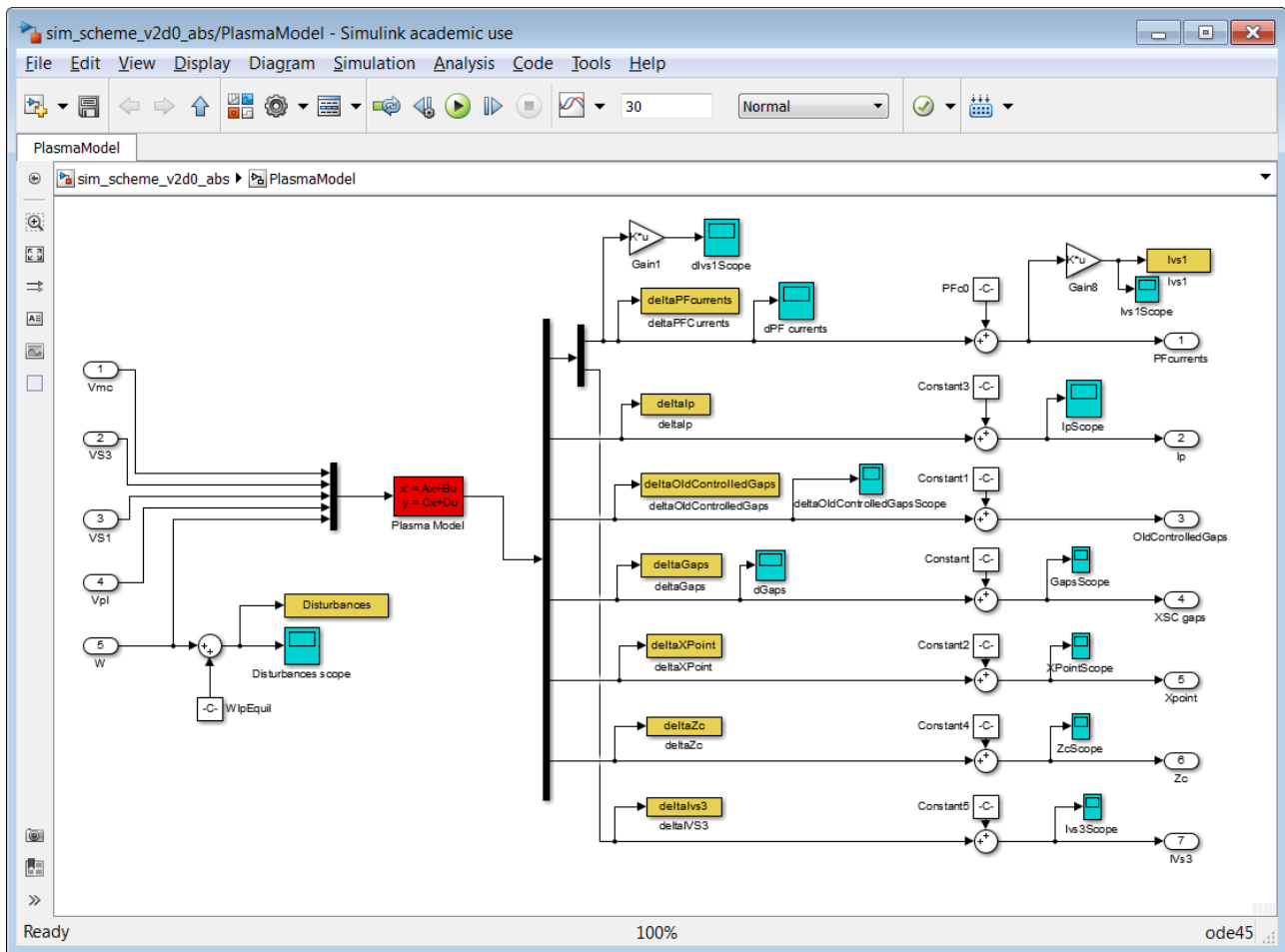


Fig. 2. Block PlasmaModel of the scheme "v2d0".

The scheme includes:

- the plasma/circuits linearized model (the state-space block "Plasma Model"),
- several sum nodes to append the operating-point offset to the outputs of the plasma linear model, in order to generate "absolute" signal values,
- a simplified model of plasma diagnostics for the plasma vertical velocity  $v_p$  and position  $z_p$  (a first-order dynamic lag filter with the time constant equal to  $7 \cdot 10^{-3}$  s is considered),
- simplified models of the power supplies for the superconductive (SC) coils VS1 and for the in-vessel (IV) ohmic coils VS3 in the block "Power Supplies Model" (a first-order dynamic lag with the time constant equal to  $7.5 \cdot 10^{-3}$  s; a delay equal to  $2.5 \cdot 10^{-3}$  s; saturations  $\pm 6$  kV and  $\pm 1.5$  kV for VS1 and VS3, respectively),
- simplified models of the main power supplies in the block "Power Supplies Model" (saturations  $\pm 1.5$  kV, except for VCS1  $\pm 3$  kV, and first-order dynamic lag with the time constant equal to 0.015 s and a delay equal to 0.015 s),
- the inner cascade control loop of the VS system in the block "Vertical VS3 controller", which aims at vertically stabilizing the plasma column,
- the outer cascade control loops of plasma current and shape control, comprising the blocks "Current Controller", "Plasma Current Controller" and "XSC Controller",

- blocks enabling the simulation of vertical displacement events (VDE), using a corresponding plasma model initial state, and H-L transitions, by injecting recorded profiles of  $\beta_p$  and  $I_i$  (BPLI) [11].

The simulation solver ode23tb is used, with relative tolerance  $10^{-5}$ .

### 3 Vertical stabilisation

For vertical stabilisation, the same variant of static output feedback (SOF) control [14] is used both in the reference scheme and with the MPC controller.

The SOF VS controller acts on the control variable  $\mathbf{u}_{VS} = [u_{VS,1} u_{VS,2}]^T$ , where:

- $u_{VS,1}$  is the voltage applied to the IV coils VS3,
- $u_{VS,2}$  is the voltage applied to the SC circuit VS1,

while it attempts to drive to zero the controlled inputs  $\mathbf{y}_{VS} = [y_{VS,1} y_{VS,2}]^T$ , where

- $y_{VS,1}$  is the VS3 power supply current,
- $y_{VS,2}$  is the plasma vertical velocity  $v_p$ .

The following feedback transfer function matrix is used

$$\mathbf{u}_{VS}(t) = \mathbf{K}_{SOF} \mathbf{y}_{VS}(t), \quad \mathbf{K}_{SOF} = \begin{bmatrix} \frac{0.00175s + 0.07}{(1/6)s + 1} & -\frac{175s + 7000}{(1/6)s + 1} \\ 0.1 & 0 \end{bmatrix} \quad (1)$$

### 4 MPC Plasma current and shape (CSC) controller

The CSC output  $\mathbf{V}_{PF}$  is the vector of the 11 voltage requests to the main power supply (main converters).

The CSC inputs include:

- the currents in the 11 superconductive coils  $\mathbf{I}_{PF}$ .
- the plasma current  $I_p$ ,
- the vector of controlled gaps  $\mathbf{g}$ .

Fig. 3 displays the simulation scheme with the MPC CSC controller. The MPC CSC controller is contained in a single block "predictiveCSC", which is shown expanded in Fig. 4. The MPC controller in the block "MPT Controller" is a tracking controller that drives the controlled outputs (CSC inputs  $\mathbf{I}_{PF}$ ,  $I_p$ , and  $\mathbf{g}$ ) to their set-point values. It is based on a reduced-order discrete-time state-space model. The states of such models do not have physical meanings, and are therefore estimated using the Kalman filter  $\text{kfCSC}^1$ , which computes state estimates ( $\hat{\mathbf{x}}$ ) based on output measurements and past controller outputs. Such a scheme may also be used with a LQ optimal controller.

A revised version of an MPC controller involving a steady-state target calculator (TC) and a dynamic controller (DC) for transient dynamics is currently under construction and is not subject of this report, which includes the state

---

<sup>1</sup> The kalman filter  $\text{kfCSC}$  is split into two blocks,  $\text{kfCSC\_ABC}$  and  $\text{kfCSC\_D}$ , to avoid a false algebraic loop warning of Simulink.



estimation scheme only. Therefore, simulations were mostly carried out with CSC in open loop, with the MPC controller removed as shown in Fig. 5. However, for the TC and the "joint" MPC schemes, the same KF is used.

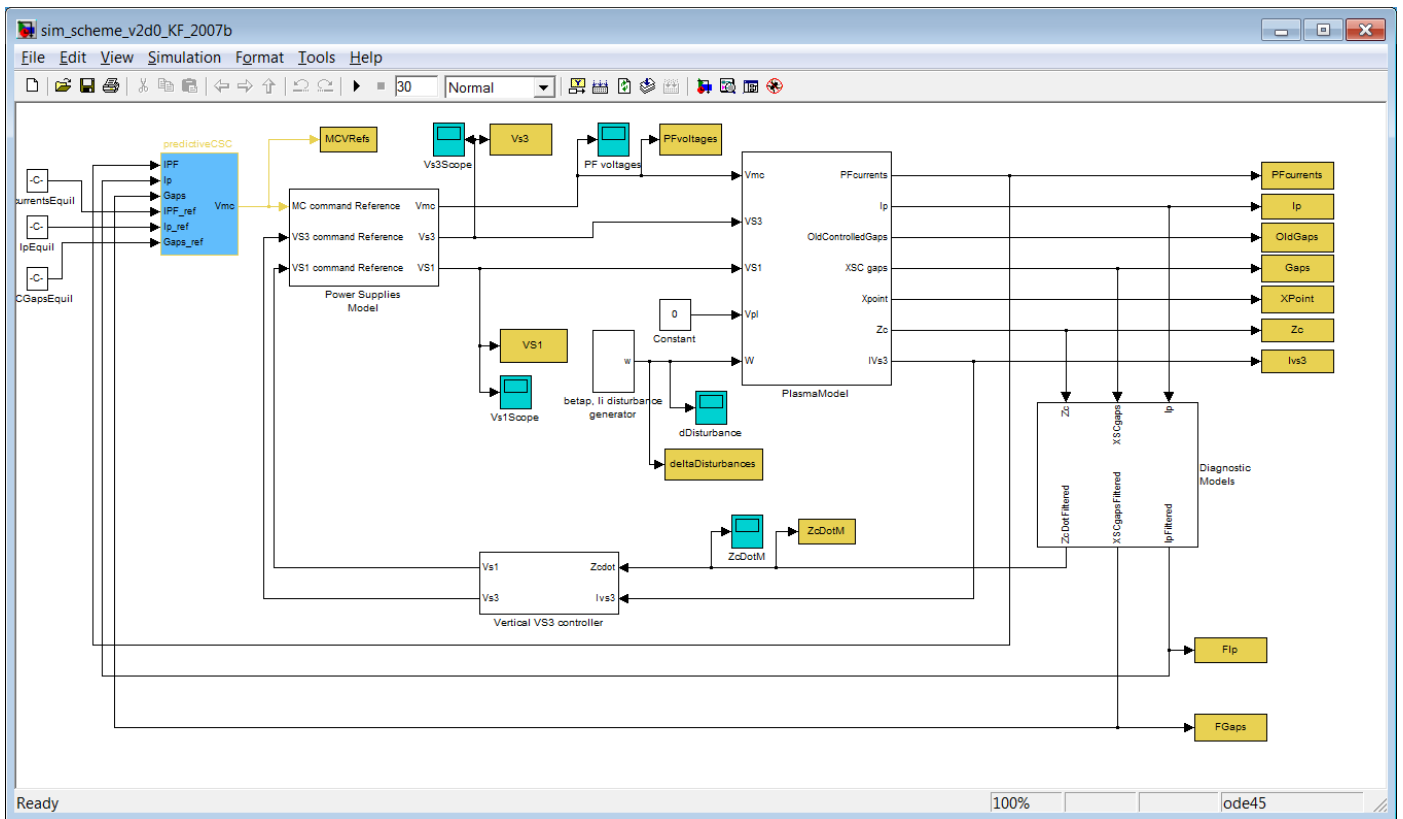


Fig. 3. Simulation control scheme with MPC CSC.

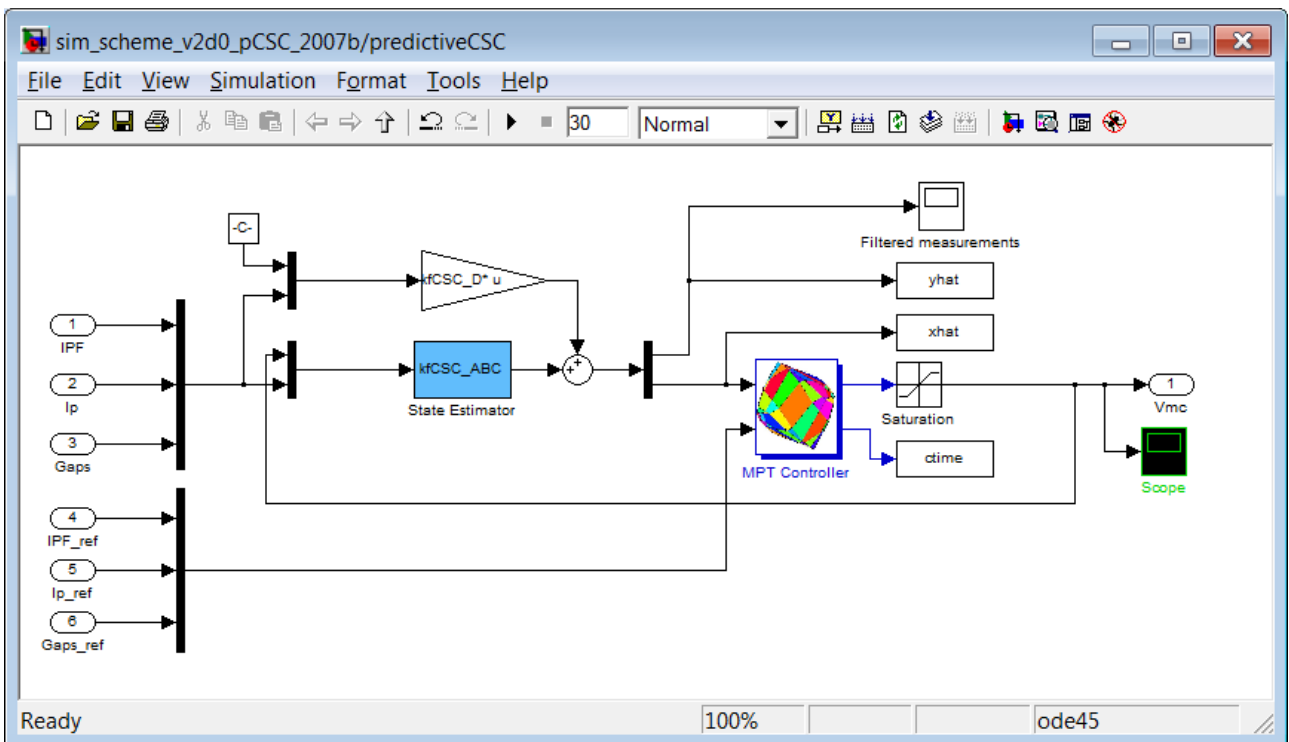


Fig. 4. Block "predictiveCSC".

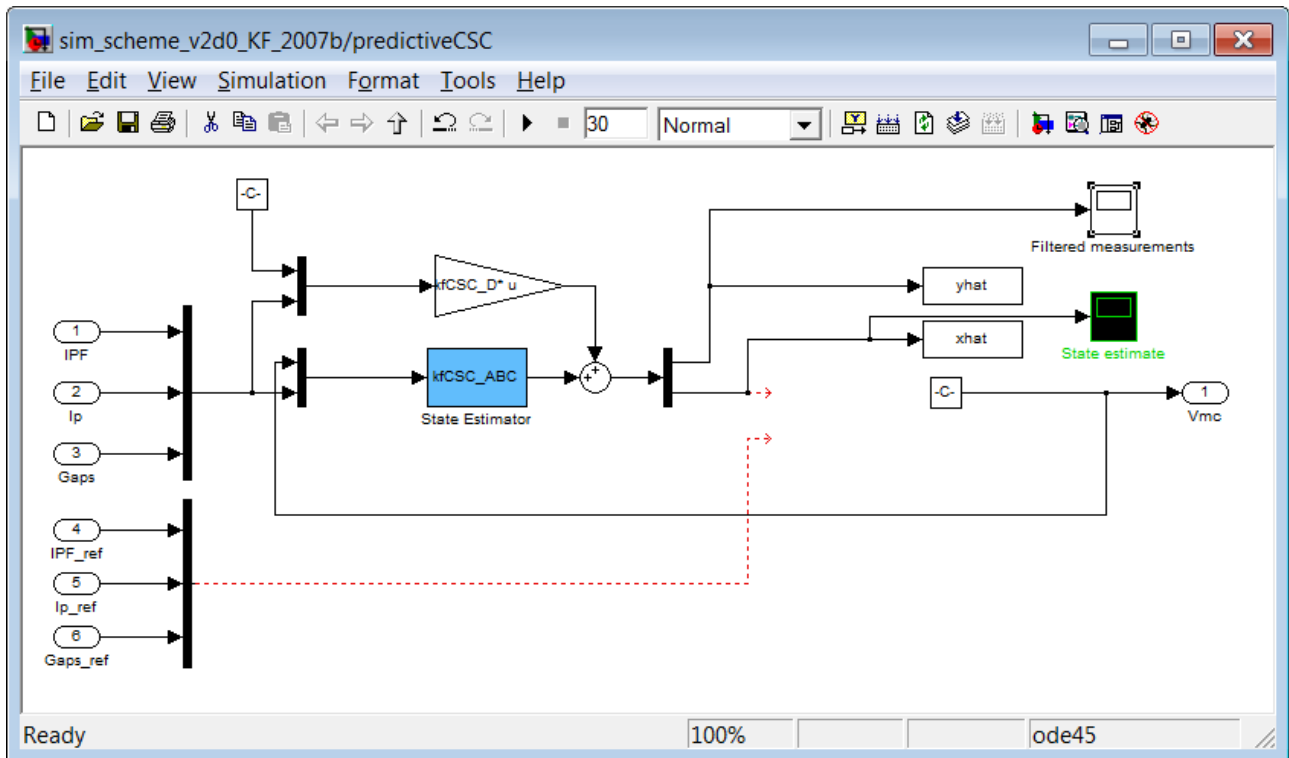


Fig. 5. Block "predictiveCSC" with KF state estimation only (no MPC controller).

## 5 Model preparation for KF and MPC

The nominal design of MPC and state estimation was based on the nominal plasma model t90 in the continuous-time. A sequence of steps is required to prepare the model in a suitable form:

- A state-space model with the appropriate inputs and outputs for the simulation scheme is formed.
- The vertical velocity output required for VS is appended.
- The simplified models of the power supplies and sensors (diagnostics) are appended.
- The SOF VS feedback is added to stabilise the unstable pole. The computed closed-loop dynamics is taken as open-loop dynamics for the outer CSC control.
- The subsystem from the process inputs  $\mathbf{u}_{\text{CSC}} = \mathbf{V}_{\text{PF}}$  to the outputs  $\mathbf{y}_{\text{CSC}} = [\mathbf{I}_{\text{PF}} I_p \mathbf{g}]^T$  for CSC is extracted.
- Any possible dynamic artifacts at very low frequencies due to numerical noise in computations must be removed using the `stabsep matlab` function, because they have adverse effects on model reduction and cause problems with the Target Calculator design. Clean integrating dynamics due to the superconducting coils are expected from all 11 process inputs  $\mathbf{u}_{\text{CSC}}$ .
- Model reduction is used to decrease the model order as much as possible without affecting the performance. Unfortunately, it is difficult to choose the appropriate order in advance, because the choice may depend on KF and MPC tuning - a better model may be required for a higher bandwidth. The effect of order reduction is illustrated with the Bode diagram in Fig. 6. Model order 60 is chosen for the moment.

### Model reduction

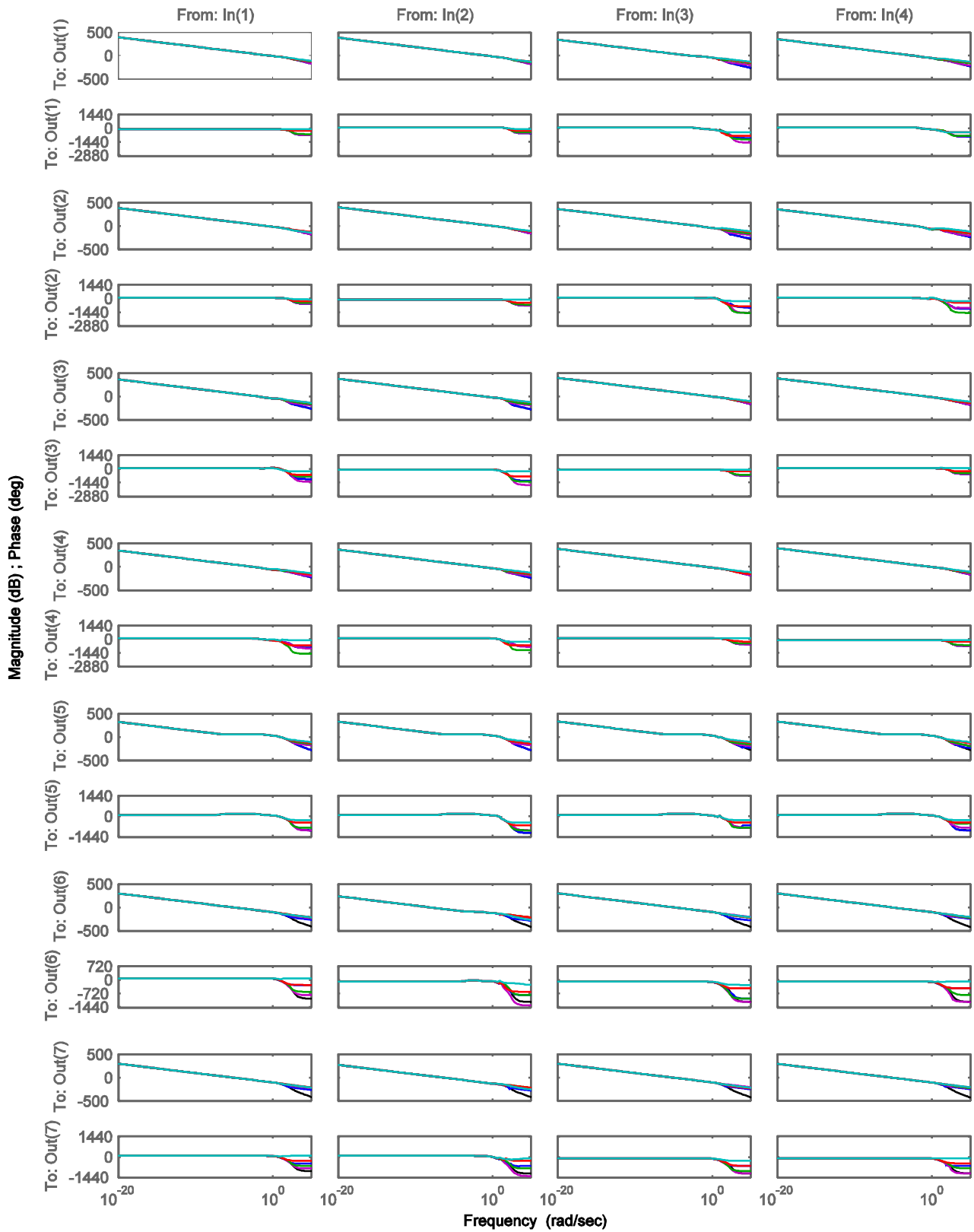


Fig. 6. Bode diagram of a subsystem of the unreduced model (black) and the reduced-order models with 129 (blue), 80 (magenta), 60 (green), 40 (red), and 20 (cyan) states. A subsystem from inputs 1, 2, 10, and 11 to outputs 1, 2, 10, 11, 12, 13, and 14 is shown.

- The base model for the MPC CSC  $\{\mathbf{A}_{CSC}, \mathbf{B}_{CSC}, \mathbf{C}_{CSC}, \mathbf{0}\}$  is finally obtained with model conversion to discrete time with the sampling time  $T_s = 0.1$  s, assuming zero-order hold. For the sake of the computational burden of MPC due to the online optimisation approach, the sampling time should be kept as long as possible without adversely affecting the performance. Stable simulation may be achieved with sampling times of several seconds, however a deterioration of performance is first observed with fast-acting disturbances which may appear in between sampling instants. However, due to slow process dynamics, the performance no longer improves much by using a sampling time faster than 0.2 s.
- The CSC should facilitate offset-free control of  $I_p$  and  $\mathbf{g}$  to zero with integral action, without set-point tracking. In our implementation, integral action is based on the *disturbance estimation* (DE) concept [13]. For the estimation of asymptotically non-zero disturbances, the base model is augmented with DE integrators at the outputs which require offset-free control. Consider the discrete-time state-space model

$$\begin{aligned} \mathbf{x}(k+1) &= \mathbf{A}\mathbf{x}(k) + \mathbf{B}\mathbf{u}(k) + \mathbf{w}(k), \\ \mathbf{y}(k) &= \mathbf{C}\mathbf{x}(k) + \mathbf{v}(k) \end{aligned} \quad (1)$$

where  $\mathbf{w}$  and  $\mathbf{v}$  are white noise signals to the state and output, respectively. DE integrator states  $\mathbf{d}$  with the associated white-noise signal  $\mathbf{w}_d$  are appended to the state  $\mathbf{x}$ , so that the augmented state is  $\mathbf{x}_a = [\mathbf{x}^T \mathbf{d}^T]^T$ , and  $\mathbf{w}_a = [\mathbf{w}^T \mathbf{w}_d^T]^T$ . The augmented system is

$$\begin{aligned} \begin{bmatrix} \mathbf{x}(k+1) \\ \mathbf{d}(k+1) \end{bmatrix} &= \begin{bmatrix} \mathbf{A} & \mathbf{0} \\ \mathbf{0} & \mathbf{I} \end{bmatrix} \begin{bmatrix} \mathbf{x}(k) \\ \mathbf{d}(k) \end{bmatrix} + \begin{bmatrix} \mathbf{B} \\ \mathbf{0} \end{bmatrix} u(k) + \begin{bmatrix} \mathbf{I} & \mathbf{0} \\ \mathbf{0} & \mathbf{I} \end{bmatrix} \begin{bmatrix} \mathbf{w}(k) \\ \mathbf{w}_d(k) \end{bmatrix} \\ \mathbf{y}(k) &= \begin{bmatrix} \mathbf{C} & \mathbf{I} \end{bmatrix} \begin{bmatrix} \mathbf{x}(k) \\ \mathbf{d}(k) \end{bmatrix} + \mathbf{v}(k) \end{aligned} \quad (2)$$

and is rewritten as

$$\begin{aligned} \mathbf{x}_a(k+1) &= \mathbf{A}_a \mathbf{x}_a(k) + \mathbf{B}_a \mathbf{u}(k) + \mathbf{w}_a(k), \\ \mathbf{y}(k) &= \mathbf{C}_a \mathbf{x}_a(k) + \mathbf{v}(k) \end{aligned} \quad (3)$$

The steady-state Kalman filter (KF)

$$\begin{aligned} \mathbf{x}_a(k/k-1) &= \mathbf{A}_a \mathbf{x}_a(k-1/k-1) + \mathbf{B}_a \mathbf{u}(k-1) \\ \mathbf{x}_a(k/k) &= \mathbf{x}_a(k/k-1) + \mathbf{M}_K [\mathbf{y}(k) - \mathbf{C}_a \mathbf{x}_a(k/k-1)] \end{aligned} \quad (4)$$

is used state estimation with the disturbance-augmented model, where  $\mathbf{M}_K$  is computed via the steady-state solution of the Riccati equation from the covariance matrices  $\mathbf{Q}_K = E\{\mathbf{w}_a \mathbf{w}_a^T\}$  and  $\mathbf{R}_K = E\{\mathbf{v} \mathbf{v}^T\}$ . The KF is used in the sense of an observer, where the diagonal elements of  $\mathbf{Q}_K$  and  $\mathbf{R}_K$  are used as tuning parameters to achieve desired dynamics.

- Another form of model augmentation is the *velocity form* (possibly combined with tracking) used to prevent offset due to the control cost when the control signal is non-zero at the steady-state.

For the velocity form, the disturbance-augmented system  $\{\mathbf{A}_a, \mathbf{B}_a, \mathbf{C}_a, \mathbf{0}\}$  is augmented again. In the velocity-augmentation, the change of the input signal  $\delta \mathbf{u}$  becomes the new input; the state expands to  $\mathbf{x}_{av} = [\mathbf{x}_a^T \mathbf{u}(k-1)^T]^T$ ; the new output is  $\mathbf{y}_{av} = [\mathbf{y}_a^T \mathbf{u}(k-1)^T]^T$

$$\begin{bmatrix} \mathbf{x}_a(k+1) \\ \mathbf{u}(k) \end{bmatrix} = \begin{bmatrix} \mathbf{A}_a & \mathbf{B}_a \\ \mathbf{0} & \mathbf{I} \end{bmatrix} \begin{bmatrix} \mathbf{x}_a(k) \\ \mathbf{u}(k-1) \end{bmatrix} + \begin{bmatrix} \mathbf{B}_a \\ \mathbf{0} \end{bmatrix} \delta \mathbf{u}(k) \quad (5)$$

$$\begin{bmatrix} \mathbf{y}_a(k) \\ \mathbf{u}(k-1) \end{bmatrix} = \begin{bmatrix} \mathbf{C}_a & \mathbf{D}_a \\ \mathbf{0} & \mathbf{I} \end{bmatrix} \begin{bmatrix} \mathbf{x}_a(k) \\ \mathbf{u}(k-1) \end{bmatrix} + \begin{bmatrix} \mathbf{D}_a \\ \mathbf{0} \end{bmatrix} \delta \mathbf{u}(k)$$

with  $\mathbf{D}_a = \mathbf{0}$  rewritten as

$$\begin{aligned} \mathbf{x}_{av}(k+1) &= \mathbf{A}_{av} \mathbf{x}_{av}(k) + \mathbf{B}_{av} \delta \mathbf{u}(k) \\ \mathbf{y}_{av}(k) &= \mathbf{C}_{av} \mathbf{x}_{av}(k) \end{aligned} \quad (6)$$

Then, the MPC controller is built using the Multi-Parametric Toolbox (MPT) [4] in the output-cost formulation, with the cost function

$$J(\delta \tilde{\mathbf{u}}) = \sum_{k=0}^{N-1} \mathbf{y}_{av,k}^T \begin{bmatrix} \mathbf{Q}_{C;y} & \mathbf{0} \\ \mathbf{0} & \mathbf{0} \end{bmatrix} \mathbf{y}_{av,k} + \delta \tilde{\mathbf{u}}_k^T \mathbf{R}_{C,\delta u} \delta \tilde{\mathbf{u}}_k \quad (7)$$

where the diagonal elements of the cost matrices for the outputs  $\mathbf{Q}_{C;y}$  and the control moves  $\mathbf{R}_{C,\delta u}$  are used as tuning parameters, and  $N = 30$  is the prediction horizon length. The control law is obtained by minimising  $J$  with respect to the vector of the future control moves  $\delta \tilde{\mathbf{u}}$  subject to constraints (currently, only control amplitude constraints  $\mathbf{u}_{\min} \leq \mathbf{u} \leq \mathbf{u}_{\max}$  are used). To reduce the computational demand, the number of free control moves is reduced from 30 to 3 using move blocking to intervals [2 2 26]. Due to the finite horizon length, the control law is computed as a least-squares problem in the unconstrained case, or as a quadratic programming problem in the constrained case [13].

## 6 KF tuning

The KF is tuned by specifying the covariance matrices  $\mathbf{Q}_K$  and  $\mathbf{R}_K$ . In theory, they may be tuned by estimating noise covariances  $E\{\mathbf{w}_a \mathbf{w}_a^T\}$  and  $E\{\mathbf{v} \mathbf{v}^T\}$ , respectively. However this is infeasible with a not-yet-existing system. Another issue is that such an optimal filtering approach leads to filtering which is mathematically optimal with respect to the defined  $l_2$  norm, however the impact of this optimality on actual control requirements are unclear. Further, it is well known that the design of an optimal filter (KF) and its dual LQ optimal controller leads to favourable properties of each and good overall performance as long as the certainty equivalence assumption holds; however the composite system may not be robust to modelling error. Loop Transfer Recovery (LTR) is one known approach to overcome the robustness issue by either matching KF tuning to the LQ controller or vice versa; though, it is not clear to apply it with augmented models. Therefore, independent tuning of the KF is possible only at the initial stage, while the final phase is carried out together with tuning the controller, where cross-validation on a set of different actual models is essential.

In practice, manual tuning is often used, using identity matrices or more general diagonal matrices. Simple identity matrices lack tuning flexibility, while considering diagonal elements individually results in an excessive number of tuning parameters. A compromise may be achieved by considering the structure of the state and output vectors and blocking related parameters together. The output vector is known to comprise elements of  $\mathbf{I}_{PF}$ ,  $I_p$  and  $\mathbf{g}$  which have different properties and value ranges. The state vector also has a particular structure when using the modal form. The last 11 elements are inherent integrating dynamics, while the others represent transient stable dynamics; the appended modes are integrating disturbance modes at the respective outputs. So, one possible structure of the covariance matrices is

$$\mathbf{Q}_K = \begin{bmatrix} k_3 \mathbf{C}\mathbf{C}^T & & & \\ & k_4 \mathbf{I}_{11} & & \\ & & k_5 \mathbf{Z}_{12} & \\ & & & k_6 \mathbf{Z}_{13:41} \end{bmatrix}, \quad \mathbf{R}_K = \begin{bmatrix} \mathbf{Z}_{1:11} & & \\ & k_1 \mathbf{Z}_{12} & \\ & & k_2 \mathbf{Z}_{13:41} \end{bmatrix} \quad (8)$$

with 6 tuning parameters  $k_1 \dots k_6$ , where  $\mathbf{Z} = \text{diag}(\mathbf{B}^T \mathbf{B})$ . With the values  $k_1 = 1$ ,  $k_2 = 1$ ,  $k_3 = 10^{-1}$ ,  $k_4 = 10^6$ ,  $k_5 = 10^2$ ,  $k_6 = 10^2$ , output estimates (dotted lines in displacement values) in Figs. 7 - 11 were obtained.

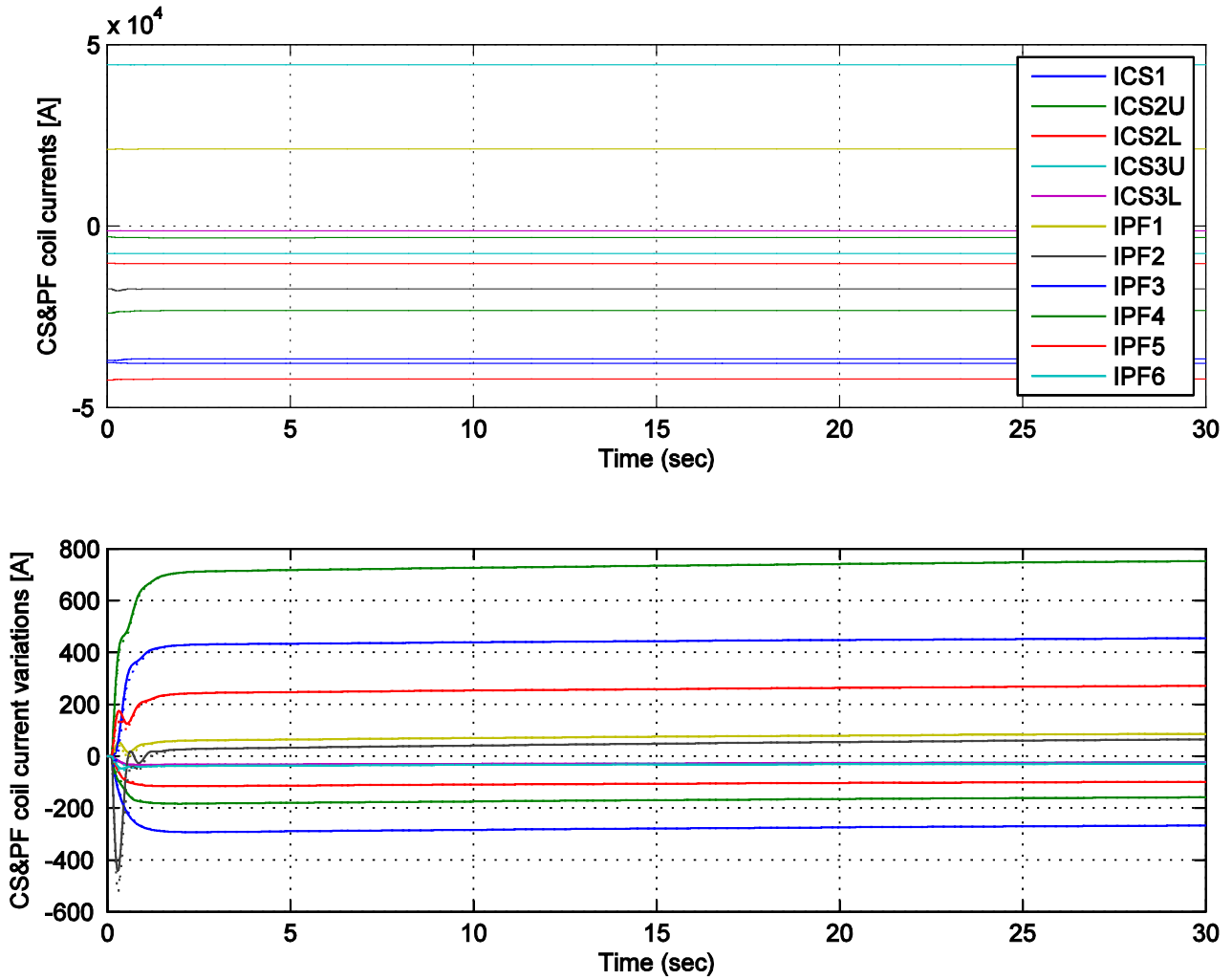


Fig. 7. Minor disruption simulation: SC&PF coil currents. Estimates are drawn with dotted lines on the lower graph only (displacement values).

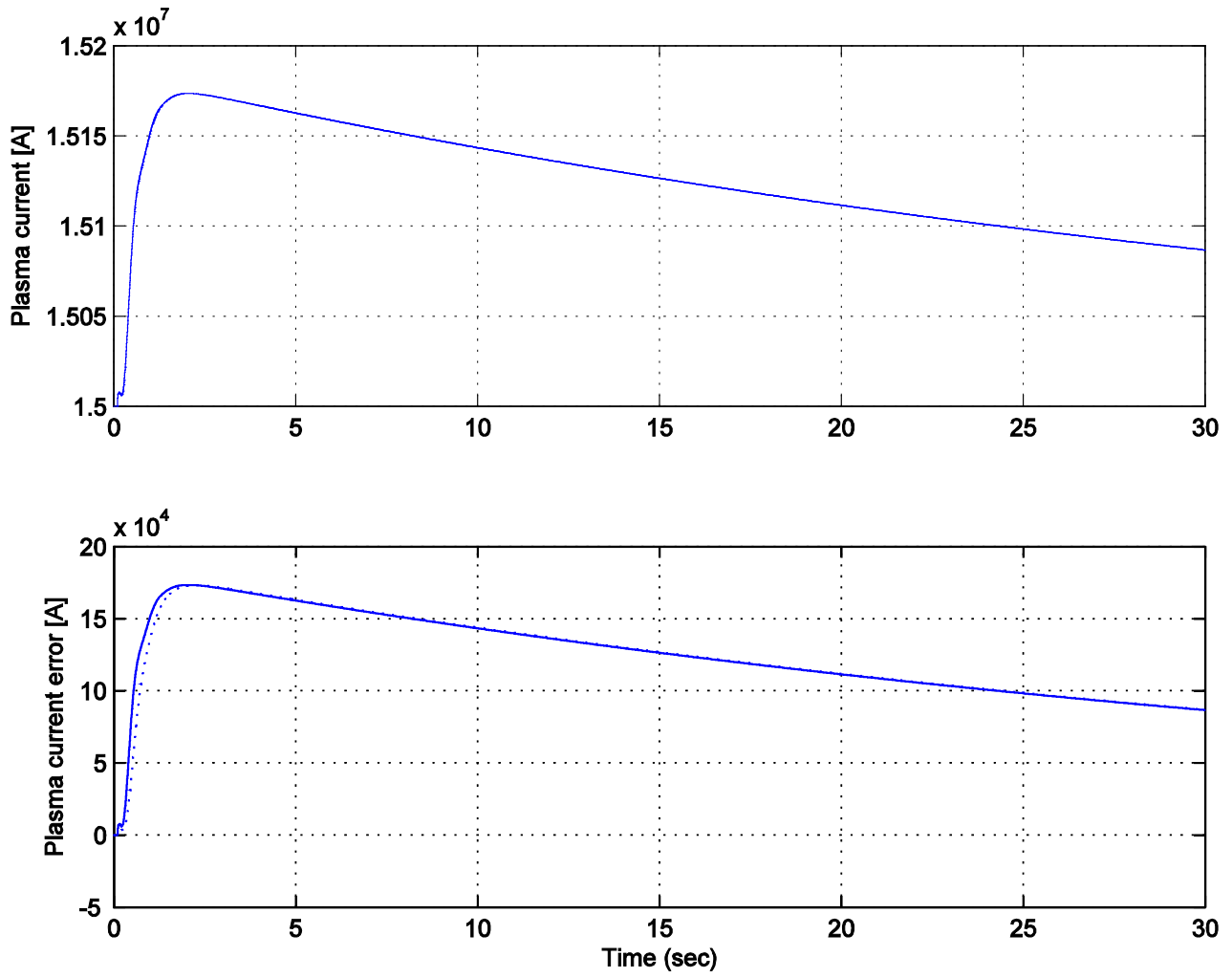


Fig. 8. Minor disruption simulation: Plasma current. Estimates are drawn with dotted line on the lower graph only (displacement values).

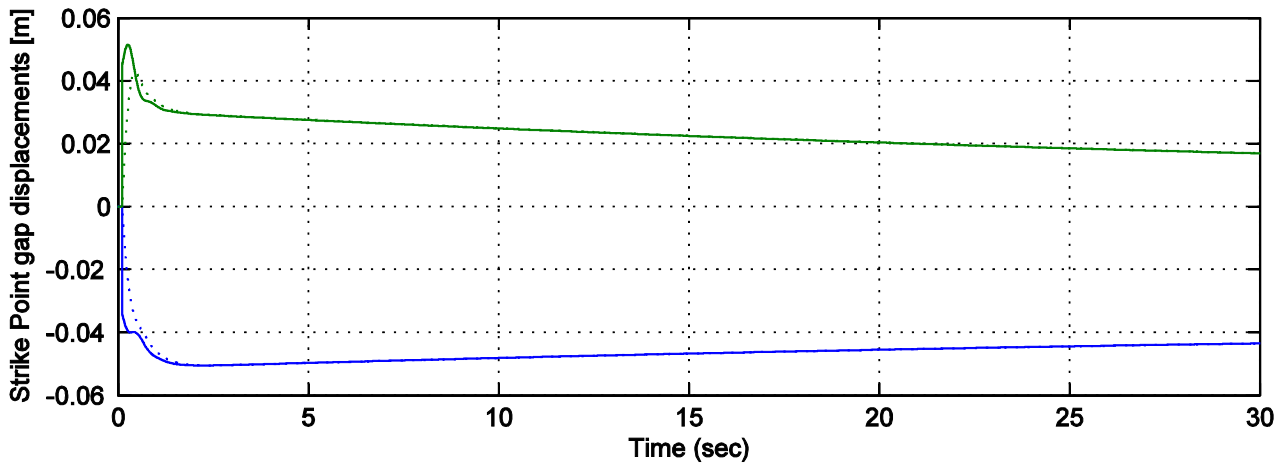
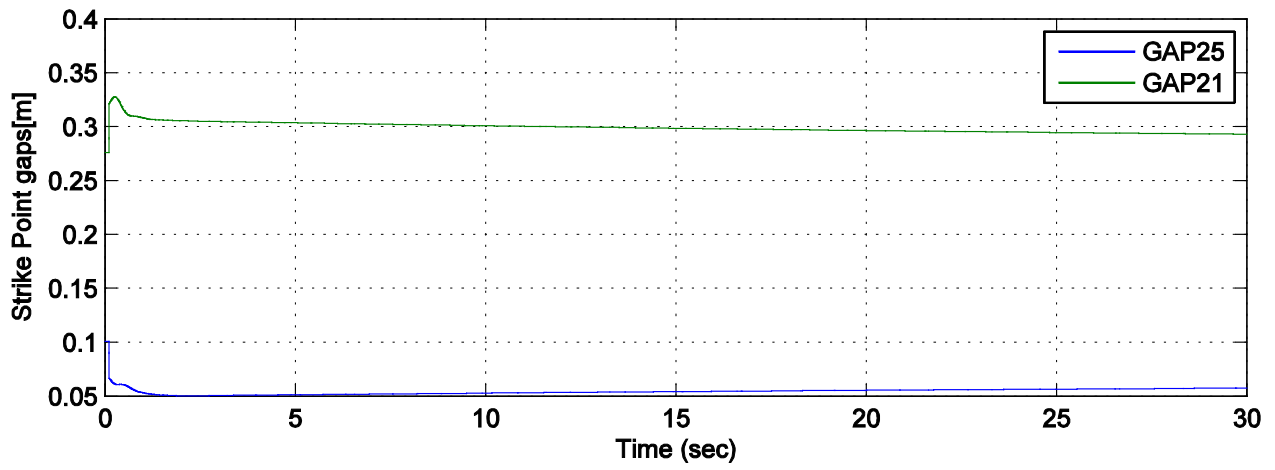


Fig. 9. Minor disruption simulation: strike points. Estimates are drawn with dotted lines on the lower graph only (displacement values).



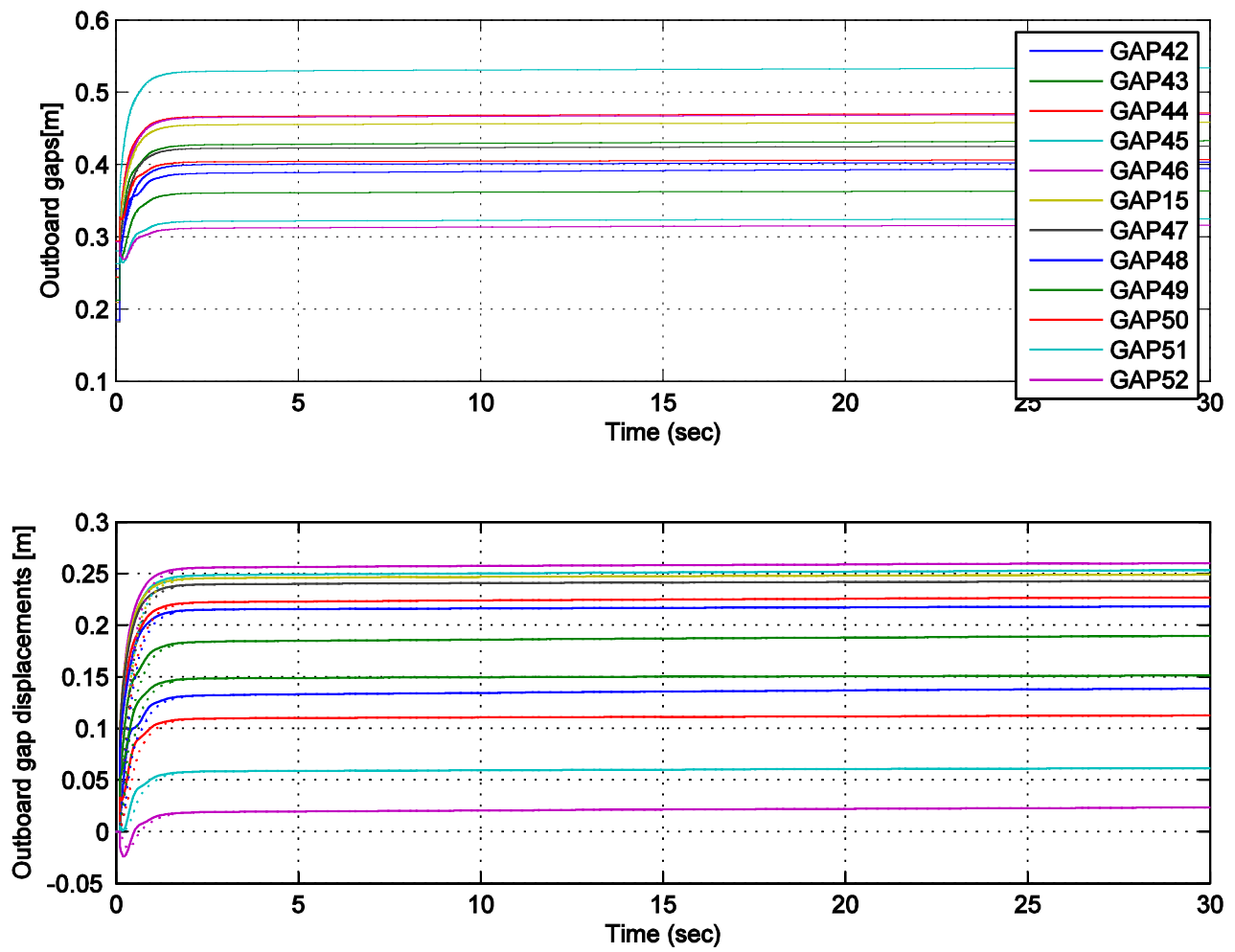


Fig. 10. Minor disruption simulation: Outboard gaps. Estimates are drawn with dotted lines on the lower graph only (displacement values).

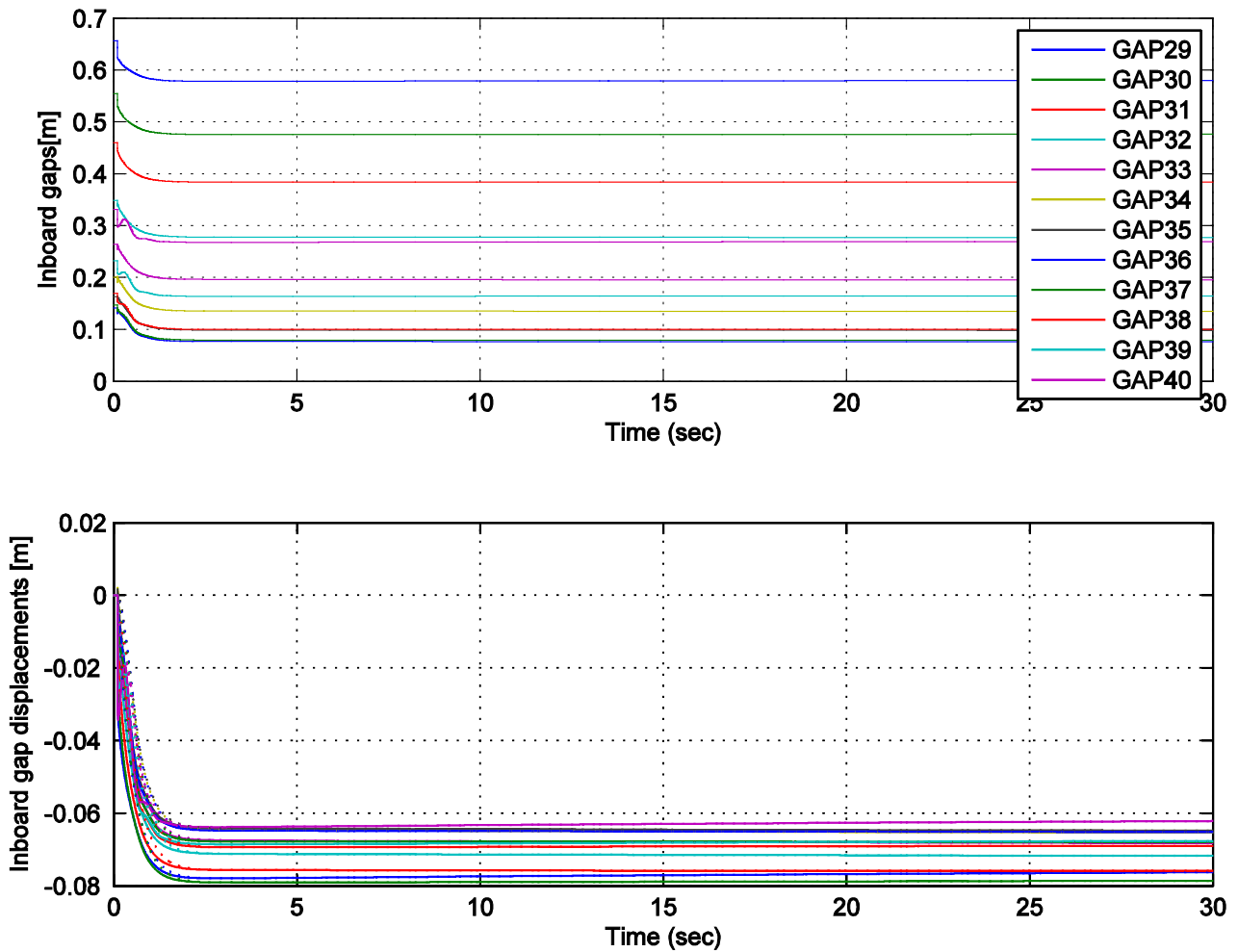


Fig. 11. Minor disruption simulation: Inboard gaps. Estimates are drawn with dotted lines on the lower graph only (displacement values).

## 7 Conclusions

In this preliminary report we describe the first steps for the design of a CSC using MPC. More specifically we have:

1. Introduced the plasma models which will be used for the design and the validation
2. Described the overall plasma plus feedback controller scheme, developed in Matlab/Simulink
3. Described the vertical controller used to stabilise the plasma
4. Described the tools needed for the MPC design. In particular we have tuned a KF for the estimation of the state of a plasma reduced order model, which produces reasonable state estimates with the model running in open loop.

## References

- [1] T. Bellizio et al., Control of elongated plasma in presence of ELMs in the JET tokamak, *IEEE T. Nucl. Sci.* **58**, 4 (2011)
- [2] A. Neto et al., Exploitation of Modularity in the JET Tokamak VS System, *Control Eng. Pract.* **20**, 9 (2012)
- [3] S. J. Qin and T. A. Badgwell, A survey of industrial model predictive control technology, *Control Eng. Pract.*, **11** (2003)
- [4] Kvasnica, M.: "*Real-time model predictive control via multi-parametric programming*". VDM verlag, Saarbrücken, 2009.
- [5] M. N. Zeilinger et al., Real-time suboptimal Model Predictive Control using a combination of Explicit MPC and Online Optimization, *IEEE Trans. Auto. Contr.*, **56** (2011) 1524–1534
- [6] E. N. Hartley et al., Predictive control using an FPGA with application to aircraft control, *IEEE Trans. Control Systems Technology*, **22**, 3 (2014)
- [7] M. Ariola and A. Pironti, An Application of the Singular Perturbation Decomposition to Plasma Position and Shape Control, *Eur. J. Control* **9** (2003) 410–420
- [8] S. Gerškšič, G. De Tommasi, Improving magnetic plasma control for ITER *Fusion Eng. Des.* **89**, 9-10 (2014) 2477–2488
- [9] R. Albanese and F. Villone, The linearized CREATE-L plasma response model for the control of current, position and shape in tokamaks, *Nucl. Fus.* **38** (5) (1998)
- [10] R. Albanese et al., Plasma response models for current, shape and position control at JET, *Fusion Eng. Des.* **66–68** (2003)
- [11] G. Ambrosino et al., Design of the Plasma Position and Shape Control in the ITER Tokamak Using In-Vessel Coils, *IEEE Trans. Plasma Science* **37** (2009)
- [12] S. Gerškšič and G. De Tommasi, Vertical stabilization of ITER plasma using explicit model predictive control, *Fusion Eng. Des.* **88**, 6-8 (2013) 1082–1086
- [13] S. Gerškšič and B. Pregelj, Tuning of a tracking multi-parametric predictive controller using local linear analysis, *IET Control Theory Appl.* **6**, 5 (2012), 1–11
- [14] G. Ambrosino et al., Plasma Vertical Stabilization in the ITER Tokamak via Constrained Static Output Feedback, *IEEE T. Contr. Syst. T.* **19**, 2 (2011)